

# Detection of subthreshold pulses for neurons with channel noise

Yong Chen\*, Lianchun Yu, and Shao-Meng Qin

*Institute of Theoretical Physics, Lanzhou University, Lanzhou 730000, China*

(Dated: December 13, 2018)

Neurons in brains are subject to various kinds of noises. Beside of the synaptic noise, the stochastic opening and closing of ion channels represents an intrinsic source of noise that affects the signal processing properties of the neuron. Here we investigated the response of a stochastic Hodgkin-Huxley neuron model to transient input pulses. We found that the response (firing or no firing), as well as the response time, is dependent on the state of the neuron at the moment when input pulse is applied. The state-dependent properties of the response is studied with phase plane analysis method. Using a simple pulse detection scenario, we demonstrated channel noise enable the neuron to detect subthreshold signals. A simple neuronal network which can marvelously enhance the pulses detecting ability was also proposed. The phenomena of intrinsic stochastic resonance is found both in single neuron level and network level. In single neuron level, the detection ability of the neuron was optimized versus the ion channel patch size(i.e., channel noise intensity). Whereas in network level, the detection ability of the network was optimized versus the number of neurons involved in.

PACS numbers: 87.19.La, 87.16.Uv, 05.40.-a, 87.16.-b, 07.05.Tp

## I. INTRODUCTION

It is well known that neurons in brains are subject to various kinds of noises. Intracellular recordings of cortical neurons in vivo consistently display a highly complex and irregular activity [1], which results from an intense and sustained discharge of presynaptic neurons in the cortical network. Studies suggest that this tremendous synaptic activity, or synaptic “noise”, may play a prominent role in neural information transmission as well as in neural information processing[2]. For example, in certain situation, through phenomena which is well-known as stochastic resonance (SR), synaptic noise facilitates information transfer or allows the transmission of otherwise subthreshold inputs[3]. Actually, SR induced by synaptic noise has been extensively studied in single neurons and neural populations both experimentally and numerically[4, 5, 6].

While the synaptic noise account for the major contribution of the noise in neural system, another significant source is noise from stochastic ion channel activities. Voltage-gated ion channels in neuronal membranes fluctuate randomly between different conformational states due to thermal agitation. Fluctuations between conducting and nonconducting states give rise to noisy membrane currents and subthreshold voltage fluctuations. Recently much attention is paid to this field and channel noise is now understood to have important effects on neuronal information processing capabilities. Studies show that channel noise changes action potential dynamics, enhances signal detection, alters the spike-timing reliability and affecting the tuning properties of the cell[7, 8, 9, 10](for review see[11]).

Detection of small signals is particularly important for animal survival[12]. Both experimental and numerical studies have found, as SR predicts, that synaptic noise can enhance the detection of subthreshold signals in nonlinear, threshold-detecting systems. However, whether channel noise can play

the same role as synaptic noise does in signal detection remains unknown. In this distribution we concentrate on the subthreshold pulse detection of neurons with channel noise. First, using the stochastic Hodgkin-Huxley (SHH) neuron model, we studied the effects of channel noise on neuron’s response properties to subthreshold pulse input. It is shown that the response of SHH neuron to subthreshold signals is state dependent. Explicitly, the higher the membrane voltage is from its resting potential, the neuron more tends to fire and the response time is shorter. This result is well explained with phase analysis method. Then, we evaluated the subthreshold signal detection ability of the SHH neuron under the scenario proposed by Cregor Wenning *et al*[13]. Wenning *et al* in their work reported that colored synaptic noise could enhance the detection of subthreshold input, but the total error is always great than 0.5. In the case of channel noise, we come to the same conclusion. This result means biological relevance of pulse detection for single neuron is questionable. Therefore, we proposed the possible way of out this predicament in the case of populations of neurons. We found that the subthreshold signal detection can be greatly enhanced with the neuronal network we proposed. We also reported in this distribution a phenomenon of intrinsic stochastic resonance, which is induced by channel noise. This intrinsic SR indicates that the best detection ability is reached when the single neuron has an optimal membrane area or the network has optimal number of neurons.

Our paper is organized as follows. In Sec. II the stochastic version of Hodgkin-Huxley neuron model is presented. In sec. III, the pulse detection scenario is illustrated. The corresponding numerical results for single neurons are shown in Sec. IV. Sec. V is devoted to enhancing pulse detection with multiple neurons. First we introduced the scheme for synchronous firing spikes to detect pulses. Then, the uncoupled and coupled cases are presented separately and the underline mechanism is discussed. A conclusion is presented in Sec. VI.

---

\*Email: ychen@lzu.edu.cn

## II. MODELS

### A. Deterministic Hodgkin-Huxley Model

The conductance-based Hodgkin-Huxley (HH) neuron model provides direct relation between the microscopic properties of ion channel and the macroscopic behavior of nerve membrane[14]. The membrane dynamics of the HH equations is given by

$$C_m \frac{dV}{dt} = -(G_K(V - V_K^{rev}) + G_{Na}(V - V_{Na}^{rev}) + G_L(V - V_L)) + I, \quad (1)$$

where  $V$  is the membrane potential.  $V_K^{rev}$ ,  $V_{Na}^{rev}$ ,  $V_L$  are the reversal potentials of the potassium, sodium and leakage currents, respectively.  $G_K$ ,  $G_{Na}$ , and  $G_L$  are the corresponding specific ion conductances.  $C_m$  is the specific membrane capacitance, and  $I$  is the current injected into this membrane patch. The conductances for potassium and sodium channel ion channel are given by

$$G_K(V, t) = \bar{g}_K n^4, \quad G_{Na}(V, t) = \bar{g}_{Na} m^3 h. \quad (2)$$

The gating variables  $n, m, h$  obey the following equations,

$$\begin{aligned} \frac{d}{dt}n &= \alpha_n(V)(1 - n) - \beta_n(V)n \\ \frac{d}{dt}m &= \alpha_m(V)(1 - m) - \beta_m(V)m \\ \frac{d}{dt}h &= \alpha_h(V)(1 - h) - \beta_h(V)h \end{aligned} \quad (3)$$

where  $\alpha_x(V)$  and  $\beta_x(V)$  ( $x = n, m, h$ ) are voltage dependent opening and closing rates and are given in Table I with other parameters used in the following simulations.

### B. Stochastic Hodgkin-Huxley Model

The deterministic HH model describes the average behavior of a larger number of ion channels. However, ion channels are stochastic devices, and for the limited number of channels, statistic fluctuations will play a role in neuronal dynamics[15]. There are usually two kinds of methods to treat the fluctuations in the ion conductances:

One so called Langevin method is to characterize the channel noise with Gaussian white noise. In this stochastic HH model, the voltage variables still obey the Eqs.(1) and (2) but the gating variables are random quantities obeying the set of stochastic different equations

$$\begin{aligned} \frac{d}{dt}n &= \alpha_n(V)(1 - n) - \beta_n(V)n + \bar{\xi}_n(t) \\ \frac{d}{dt}m &= \alpha_m(V)(1 - m) - \beta_m(V)m + \bar{\xi}_m(t) \\ \frac{d}{dt}h &= \alpha_h(V)(1 - h) - \beta_h(V)h + \bar{\xi}_h(t) \end{aligned} \quad (4)$$

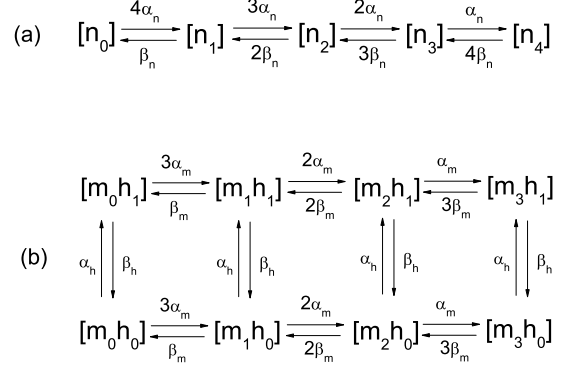


FIG. 1: Kinetic scheme for a stochastic potassium channel (a) and sodium channel (b).  $n_4$  and  $m_3h_1$  are open states, while the other states are no-conducting.

where the variables  $\bar{\xi}_n(t)$ ,  $\bar{\xi}_m(t)$ , and  $\bar{\xi}_h(t)$  denote Gaussian zero-mean white noise with

$$\begin{aligned} \langle \bar{\xi}_n(t) \bar{\xi}_n(t') \rangle &= \frac{2}{N_K} \frac{\alpha_n(V)(1 - n) - \beta_n(V)n}{2} \delta(t - t') \\ \langle \bar{\xi}_m(t) \bar{\xi}_m(t') \rangle &= \frac{2}{N_{Na}} \frac{\alpha_m(V)(1 - m) - \beta_m(V)m}{2} \delta(t - t') \\ \langle \bar{\xi}_h(t) \bar{\xi}_h(t') \rangle &= \frac{2}{N_{Na}} \frac{\alpha_h(V)(1 - h) - \beta_h(V)h}{2} \delta(t - t'), \end{aligned} \quad (5)$$

where  $N_K$  and  $N_{Na}$  are the total number of potassium and sodium channels. Note that with this method, a restriction should be included to guarantee that  $n, m$  and  $h$  do not leave the unit interval[0,1]. It has been argued that the Langevin method could not reproduce accurate result (see ref. [16] for detail). But it is useful for us to analysis our model in  $V - m$  phase plane because the trajectory of the phase point prior to a spike entails major changes in the variables  $V$  and  $m$  but during the same epoch the variables  $n$  and  $h$  are practically unchanged [17].

In the other method, the ion channel stochasticity is introduced by replacing the equations describing the ion channel conductances with explicit voltage-dependent Markovian kinetic models for single ion channels[8, 11]. As shown in Fig. 1, the  $K^+$  can channels exist in five different states and switch between them according to voltage depended transition rates (identical to the original HH rate functions).  $n_4$  labels the single open state of the  $K^+$  channel. The  $Na^+$  channel kinetic model has 8 states, with only one open state  $m_3h_1$ . Thus the voltage-dependent conductances for the potassium and sodium channels are given by

$$G_K(V, t) = \gamma_K [n_4] / S, \quad G_{Na}(V, t) = \gamma_{Na} [m_3h_1] / S, \quad (6)$$

where  $\gamma_K$  and  $\gamma_{Na}$  are the single-channel conductances of potassium and sodium channels.  $[n_4]$  refers to the number of open potassium ion channels and  $[m_3h_1]$  refers to the number of open sodium ion channels.  $S$  is the membrane area of the neuron.

TABLE I: Parameters and Rate Functions Used in the Simulations.

$C_m$	Specific membrane capacitance	$1\mu F/cm^2$
$V_K^{rev}$	Potassium reversal potential	$-77mV$
$V_Na^{rev}$	Sodium reversal potential	$50mV$
$V_L$	Leakage reversal potential	$-54.4mV$
$\gamma_K$	Potassium channel conductance	$20pS$
$\gamma_{Na}$	Sodium channel conductance	$20pS$
$G_L$	Leakage conductance	$0.3mS/cm^2$
$\rho_K$	Potassium channel density	$20/\mu m^2$
$\rho_{Na}$	Sodium channel density	$60/\mu m^2$
$\alpha_n$		$\frac{0.01(V+55)}{1-e^{-(V+55)/10}}$
$\beta_n$		$0.125e^{-(V+65)/80}$
$\alpha_m$		$\frac{0.1(V+40)}{1-e^{-(V+40)/10}}$
$\beta_m$		$4e^{-(V+65)/18}$
$\alpha_h$		$0.07e^{-(V+65)/20}$
$\beta_h$		$\frac{1}{1+e^{-(V+35)/10}}$

The numbers of open potassium and sodium ion channels at a special time  $t$  is determined in the following way: if the transition rate between state  $A$  and state  $B$  be  $r$  and the number of channels in these states be  $n_A$  and  $n_B$ . Then, the probability that a channel switches within the time interval  $(t, t + \Delta t)$  from state  $A$  to  $B$  is given by  $p = r\Delta t$ . Hence, for each time step, we determine  $\Delta n_{AB}$ , the number of channels switch from  $A$  to  $B$ , by choosing a random number from a binomial distribution,

$$P(\Delta n_{AB}) = \binom{n_A}{\Delta n_{AB}} p^{\Delta n_{AB}} (1-p)^{(n_A-\Delta n_{AB})}. \quad (7)$$

Then we update  $n_A$  with  $n_A - \Delta n_{AB}$ , and  $n_B$  with  $n_B + \Delta n_{AB}$ . To make sure that the number of channels in each state is positive, we update those number sequentially, starting with the process with the largest rate and so forth[16].

The noisiness of a group of channels can be quantified by the coefficient of variation (CV) of membrane current. Under assumptions of stationarity ( $V$  is fixed),  $CV = \{(1-p)/np\}^{1/2}$ , where  $n$  is the number of channels and  $p$  is the probability for each channel to open. Thus the noisiness of a given population of voltage-gated channels is proportional to  $n^{1/2}$ [11]. In this study, we introduce membrane area  $S$  as a control parameter of channel noise level. If the ion channel density is given, the channel noise level decreases as the membrane area increases. The numerical integration of the stochastic equations of both occupation number method and Langevin method are carried out by using forward Euler integration with a step size of 0.01ms. The parameters used in the simulations are listed in Table I. The occurrences of action potentials are determined by upward crossings of the membrane potential at a certain detection threshold of 10mV if it has previously crossed the reset value of -50mV from below.

### III. THE RESPONSE OF SHH NEURON TO TRANSIENT INPUT PULSE

In this study, we formulate the signal detection task a neuron can perform into a special case, which is to detect a tran-

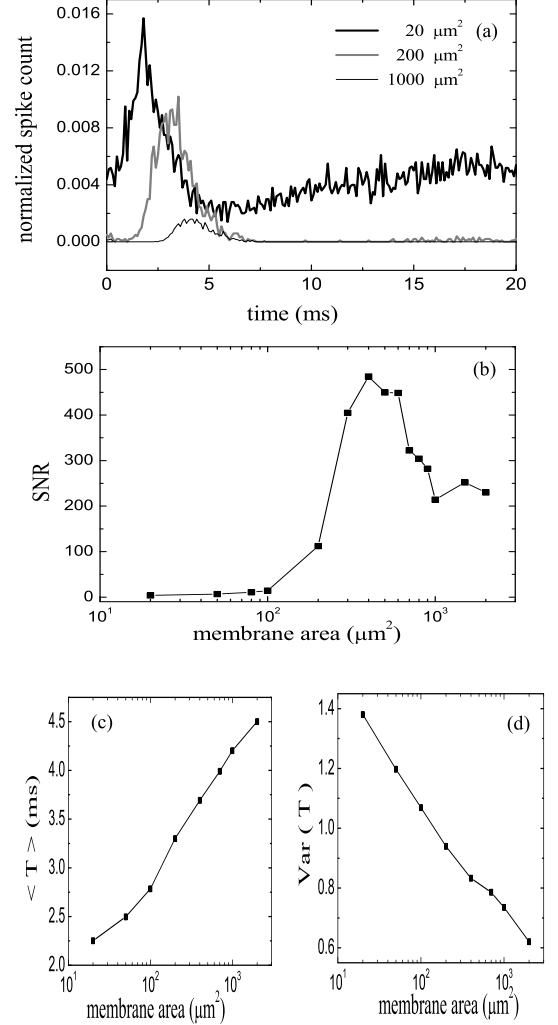


FIG. 2: The response property of SHH neuron to the subthreshold transient input pulses: (a) The PSTH of SHH neuron with different membrane area. (b) The SNR as a function of membrane area. (c) The mean response time as a function of membrane area. (d) The second moment of response time as a function of membrane area.

sient subthreshold input pulse. This special case of computational task has received increasing attention in the recent years[19, 20](see [13] for more references). First, to see how the SHH neurons response to the subthreshold transient input pulses, we applied a transient input pulses with width  $\delta t = 0.1$  ms and strength  $I_0 = 5 \mu A/cm^2$  and calculated the post-stimulus time histogram (PSTH). As seen in Fig. 2(a), the time after stimulus onset is divided into a number of bins ( $binsize = 0.1ms$ ). The stimulus is then presented repeatedly ( $n=5000$ ). The normalization of number of spikes observed in each bin to the total number of stimuli and to the bin size, produces the statistics. In this way, the PSTH gives the firing

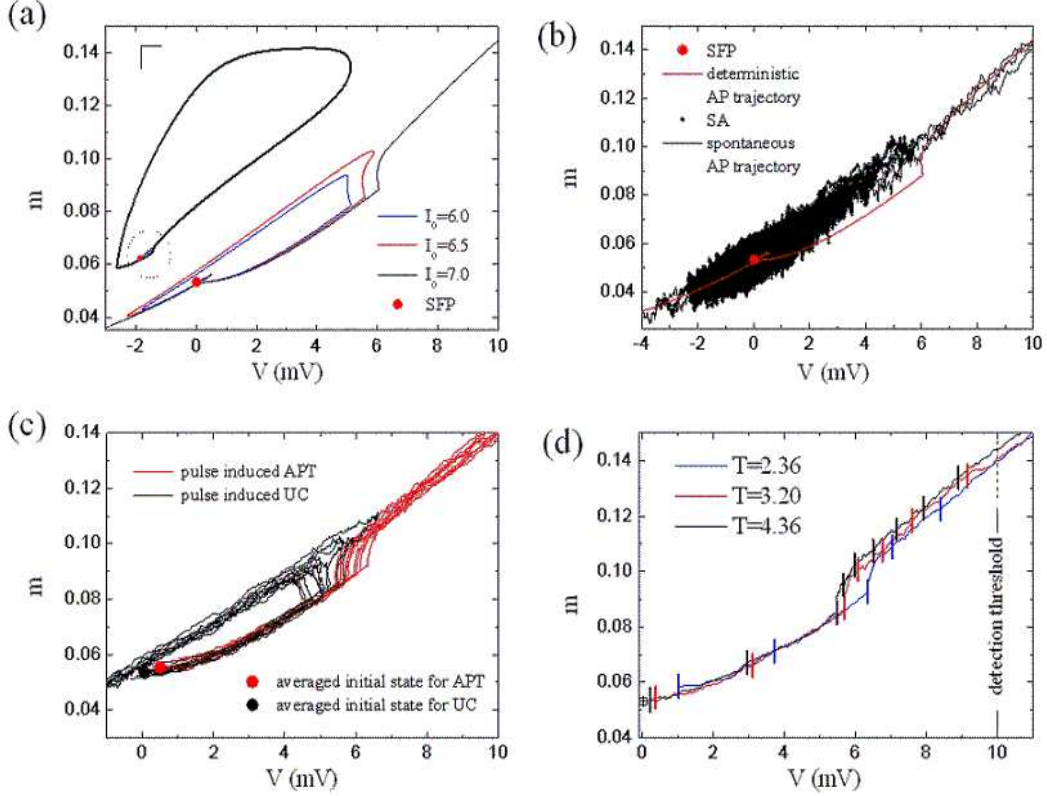


FIG. 3: The phase plane analysis of mechanism underline the response property of SHH neuron with Langevin somulation: (a) the APT and UC of a noise-free HH neuron in the phase plane. Inset: the overall APT and the position expanded in (a)(marked with dashed circle). (b) the SA and the spontaneous APT with membrane area=  $100\mu m^2$ . (c) the noise induced APT and UC, with membrane area=  $1000\mu m^2$ . (d) equitime labelling analysis of the response time to different initial state.

rate or the distribution of the firing probability per unit time as a function of time[21]. It is seen that when the neuron is stimulated by subthreshold pulses, there is a sharp increase of firing probability over the spontaneous firing level. Those peaks over the average levels indicate the sensitivity of neurons to the transient input pulses. The higher the peak is, the more sensitive of the neurons to stimuli. The baselines indicate the average level of spontaneous firing due to channel noise. The higher the baseline is, the more spontaneous spikes occur. It is seen that as the membrane area increased, the heights of both the peaks and the baselines are reduced, which means the sensitivity of neurons to subthreshold signals as well as the channel noise induced spontaneous firing is reduced with the decreasing of channel noise intensity.

To find the range of membrane area with which the neuron is more sensitive to pulse than channel noise perturbation

so that the detection task for the neuron is possible to carry out, we defined and computed the SNR (signal-to-noise ratio) as the ratio of the increased firing probability in response to the input pulses and the probability for spontaneous firing in response to channel noise[21]. As seen in Fig. 2 (b), when membrane area is smaller than  $100\mu m^2$ , SNR remains small. With the increasing of membrane area, SNR increases rapidly. However, further decreasing membrane area leads to the decreasing of SNR. Clearly, there exists stochastic resonance. This so called intrinsic SR, which appears without external noise sources, seemingly rooted in the collective properties of optimally selected ion channel assemblies. Thus, the SR indicates the existence of an optimal membrane area with which the neuron has best performance in signal detection task. In our case, the optimal value of membrane area is around  $400\mu m^2$ .

We also noticed from the Fig. 2(a) that given the membrane time, the response time of the SHH neuron is not deterministic, but follows a certain distribution. What's more, as the membrane area increases, the peak moves rightward, indicating the response time to the pulses is delayed as noise intensity decreases. To characterize this temporal property of the SHH neuron, we calculated the mean response time  $\langle T \rangle$  and the variance  $Var(T)$  corresponding to different membrane area. It is seen from (c) and (d) of Fig. 2 that as membrane area increases,  $\langle T \rangle$  increases, whereas  $Var(T)$  declines. What's more, the increasing  $\langle T \rangle$  as well as the decreasing of  $Var(T)$  is nearly in an exponential way. This phenomenon implies that the time to first spike, which may be important in timing coding of neurons, was also influenced by channel noise[17, 18].

To investigate the underline mechanism of SHH neuron responding to transient input pulses, we performed the phase plane analysis with the Langevin simulation model described above. We also set  $\delta T$  and  $I_0$  for the input pulses as  $1ms$  and  $6mA/cm^2$  for better analysis concern. Fig. 3(a) show the stable fixed point(SFP), the action potential trajectory(APT) and the unstable circles (UC) corresponding to different input pulse intensities in a noise free HH model. The inset in Fig. 3(a) shows the whole APT and in the rest plots only the APTs around the SFP (marked by the dashed circles) are shown. It is seen that there is a threshold for the system. The larger the intensity of the input pulses, the further the system will be displaced from the SFP. If the system is displaced by the input pulse across the threshold from the SFP, it will jump on the APT, evolves along it and back to the SFP, thus an action potential is generated. Otherwise the system will jump on and evolve along a relative smaller unstable circle to the SFP (the colored curves), thus only cause subthreshold membrane potential fluctuation. When the channel noise is involved, the system is not stay on the original SFP but fluctuates around the vicinity of the SFP, which we call the stable area (SA, the black area in Fig. 3(b)). And occasionally the system will be perturbed by noise across the threshold then it evolve along a stochastic AP trajectory thus a spontaneous action potential occurs. If the membrane area is smaller, then the SA is larger, thus it is easier for the system to reach the AP trajectory with the noise perturbation, giving more spontaneous firings (not shown).

To understand how the system response to the pulse input in the small noise situation, we traced ten trajectories for the pulse induced firing and no firing case respectively. As shown in Fig. 3(c), if noise is small, when the input pulse is applied, the system will be displaced to an area around the threshold. Then after the stimulus is removed, the system will jump onto the APT to generate a spike or onto the UC and return back to the SA. It is seen that the jump is random, and the more right the state before jumping is in the phase plane, the more possible for it to jump onto the APT. And the more left the state before jumping is, the more possible for the system to jump onto the UC. Since our discussion is limited into the small noise case, the noise does not affect the length of the pulse displacement, so the state position of the jumping area is decided by the initial position right before the input pulse

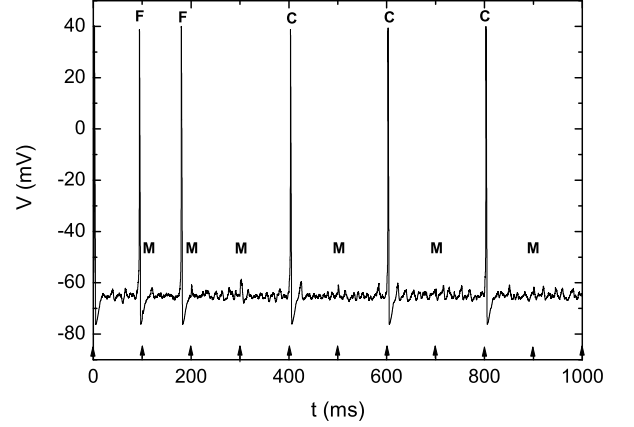


FIG. 4: Trace of the membrane potential of the SHH neuron for transient input pulses with width of  $0.1ms$  and height of  $5 \mu A/cm^2$ . The time of occurrence for pulses are marked by arrowheads on the  $x$  axis.  $C$ : the incidences that the pulse is correctly detected by the neuron;  $M$ : the incidences that the neuron does not respond to the pulse;  $F$ : the incidences that a spike occurs in the absence of a pulse.

applied. In Fig. 3(c), we also plotted the averaged initial position corresponding to the firing and no firing case. It is seen that the initial position for the firing case is right to it for the no firing case. Thus we conclude that the response of the SHH system to the input pulse is state dependent, the higher the membrane voltage before input pulse applied, the more likely for the neuron to fire a spike.

Using equitime labeling method, we also investigated the mechanism of the temporal response property of the SHH neuron. As shown in Fig. 3(d), the APTs corresponding to different response time are traced and labeled with bars separated equally by  $0.5ms$ . The most left bars indicate the time when the input pulses is applied, and the dashed line indicates the time when the spikes are detected. It is seen that if the system is displaced from the position with higher value of membrane voltage, it will reach the position closer to the detection threshold. What's more, it will jump onto the outer side APT on which the system moves quicker than the inner side APT, giving a shorter response time to the input pulse. It is reasonable to deduce that when the noise is smaller, the SA is further from the detection threshold and smaller. The longer distance from the detection in the phase plane gives shorter response time and smaller area gives less fluctuation of the response time, as (b) and (c) of Fig 2 have reflected.

#### IV. THE PERFORMANCE OF PULSE DETECTION

Here, we use the pulses detection scenario proposed by Gregor Wenning, et al, which is concerned with a detection task as a simple computation a neuron can perform[13].

The input  $I_{stim}$  is modeled as a series of narrow rectan-

gular current pulses with width  $\delta t = 0.1$  ms and strength  $I_0 = 5 \mu A/cm^2$  as before. As shown in Fig.4, the input pulse train (the arrowheads on the  $x$  axis) is regular with a large time interval  $\Delta t$  ( $=100$ ms) compared to the membrane time constant, so that the preceding pulse has no significant influence on the following one. In such an arrangement, the SHH neuron has three different responses to the pulse train which consists of  $n$  equidistant pulses:

1) The neuron generates an action potential immediately after a pulse presented (marked by **C** in Fig.4), which means it correctly detected the pulse. We define  $P_c$  as the fraction of correctly detected pulse, which is the total number of correctly detected pulses, divided by the total number of input pulses.

2) The neuron fail to fire a spike immediately after the pulse is presented (marked by **M** in Fig.4). If we define  $P_m$  as the fraction of missed pulses, then we have  $P_m = 1 - P_c$ .

3) The neuron fires a spike in the absence of a pulse (a false positive event, marked by **F** in Fig.4). A deterministic HH neuron won't fire spikes if the stimulus is not applied or it is below the threshold. However, when the channel noise is concerned, the stochastic effects give rise to spontaneous spiking. To describe the effect of those spontaneous firing spikes on the subthreshold pulse detection task, the total number of false positive events, divided by the total number of input pulses, is denoted as  $P_f$ . Note that  $P_f$  can easily exceed 1.

In order to quantify the neuron's response to the pulse train we define the total error  $Q$  for the pulse detection as the sum:

$$Q = P_m + P_f \quad (8)$$

Note that for longer intervals  $\Delta T$  but fixed  $n$  more false positive events are likely to occur, so that the total error grows with increasing  $\Delta T$ .

To evaluate the performance of pulse detection task of the SHH neuron with small and large membrane area under the above mentioned scenario, we plot  $P_c$ ,  $P_f$  and  $P_m$  as a function of the membrane area as shown in Fig. 5(a). It is seen that  $P_c$  decreases nearly exponentially as the membrane area is increased. Since  $P_c + P_m = 1$ , as  $P_c$  decreases with increasing membrane area, the fraction of missed pulse  $P_m$  increases. When membrane area is rather large, i.e, in the deterministic situation,  $P_c$  equals zero, thus  $P_m$  equals one. As can be seen from Fig. 5, when membrane area is small, because the spontaneous firing rate is rather high, the fraction of false positive  $P_f$  is larger than  $P_c$ . However, with the increasing of membrane area, the spontaneous firing rate decrease, so does the  $P_f$ . It is seen that  $P_f$  drops more quickly than  $P_c$ . As a result,  $P_c$  become large than  $P_f$  when membrane area is between  $100 \mu m^2$  to  $200 \mu m^2$ . When membrane area is very large, the spontaneously fired spikes due to channel noise is very rare, which gives a rather small value of  $P_f$ . The total error  $Q$  as a function of the membrane area is also plotted in Fig. 5(b). As the membrane area is increased, due to the rapid dropping of  $P_f$ , the total error  $Q$  drops rapidly. The minimal value for  $Q$  is 0.8746 at  $S = 300$ . After that, because the major contribution to total error  $Q$  comes from the fraction of missed pulses, with the further increasing of membrane area,  $Q$  increases and approaches 1. It is obviously that the total error is minimized versus the membrane area of the neuron. The minimal value

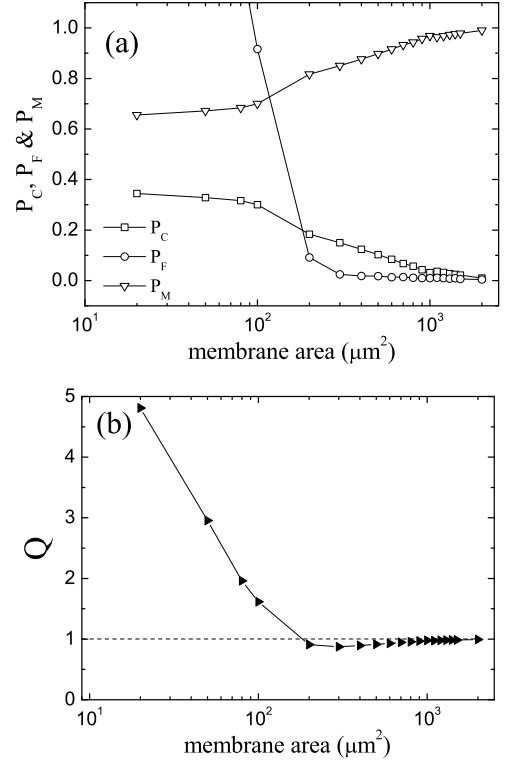


FIG. 5: The performance of a single neuron in subthreshold pulse detection task. (a)  $P_c$ ,  $P_m$  and  $P_f$  as a function of membrane area. (b) total error  $Q$  as a function of membrane area.

for  $Q$  is 0.8746 at  $S = 300$ . However, this value is larger than 0.5, which means pulses can not be reliably detected by single neuron.

As have discussed above, a single neuron has a limited capability for subthreshold signal detection. However, in real neural systems, there are a number of neurons rather than single neuron to accomplish certain tasks. Moreover, those neurons work cooperatively through synaptic coupling. Among various spatiotemporal spike patterns, synchronous firing has been most extensively studied both experimentally and theoretically[22, 23].

Now, we consider a neural network as shown in Fig. 6. The front layer of the network is composed of globally coupled identical neurons with channel noise. The coupling term has the form of an additional current  $I_{couple}$  added to the equation for the membrane potential (Eq. 1). For the  $i$ th neuron, it takes the form

$$I_{couple} = \frac{\varepsilon}{N} \sum_{j=1}^N (V_j - V_i), \quad (9)$$

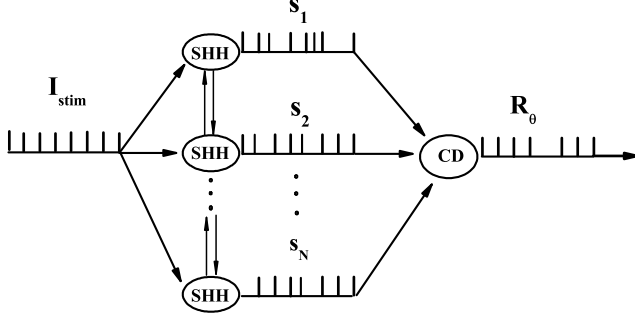


FIG. 6: A schematic diagram of pulses detection with multiple neurons.  $I_{stim}$  is the input pulse train.  $S_i$  is the output spike train of the  $i$ th SHH neuron for  $i = 1, 2, \dots, N$ . CD is the coincidence detector neuron and  $R_\theta$  is its output spike train with synchronous firing detecting threshold  $\theta$ . Here demonstrates the case of  $\theta = 2$ .

where  $\varepsilon$  is the coupling strength and  $V_i$  is the membrane potential of the  $i$ th neuron for  $i = 1, \dots, N$ . In this study,  $\varepsilon = 0.005$  so the neurons are weakly coupled. The membrane area of each SHH neuron is set as  $200\mu m^2$ . Each SHH neuron in the network receives the common subthreshold pulse input train as in the single neuron case. The output spike trains of those neurons  $S_i$ ,  $i = 1, 2, \dots, N$ , are taken as the input of a so-called coincidence detector neuron. The coincidence detector neuron is excited if it detects spikes from more than  $\theta$  neurons within a coincidence time window  $\rho$  ( $= 5$  ms). Thus,  $\theta$  is the threshold of the coincident detector neuron. After firing, the coincidence detector neuron enters in a refractory period of 5 ms. Given the input spike trains  $S_i$  ( $i = 1, 2, \dots, N$ ), the output spike train  $R_\theta$  of coincidence detector neuron is determined by its threshold  $\theta$ . We define  $P_C^\theta$  and  $P_F^\theta$  as the fraction of correct detection and false reporting of the network with coincidence detection threshold  $\theta$  respectively. In the same way,  $Q^\theta$  is defined as the total error of the network with coincidence detection threshold  $\theta$ .

When multiple neurons are applied to detect the subthreshold pulse trains, we find that the ability of correct detection is highly enhanced. Panel (a) of Fig. 7 shows  $P_C^\theta$  as a function of the number of SHH neurons  $N$  for the case of  $\theta = 1, 2, 3$ , respectively. It is seen that as  $N$  increases,  $P_C^\theta$  increases until perfect detection are achieved ( $P_C^\theta = 1$ ). However, the enhancement of  $P_C^\theta$  is at the cost of unexpected increasing of  $P_F^\theta$ . As shown in panel (b), with increasing the number of SHH neurons,  $P_F^\theta$  also increases. Note that  $P_F^\theta$  can exceed 1 as  $N$  increases. For certain  $\theta$ , compared with the corresponding curves in panel (b), the  $P_F^\theta$  curves are more rightward. So, if  $N$  is too small, the correct detection will not be greatly enhanced though  $P_F^\theta$  is low. Whereas if  $N$  is too large, better correct detection can be achieved, however, it is at the cost of high  $P_F^\theta$ . Therefore, we must find the optimal  $N$  with which the network performances signal detection task.

Panel (c) of Fig. 7 shows the total error as a function of the number of neurons  $N$  for different  $\theta$ . It is interesting to find

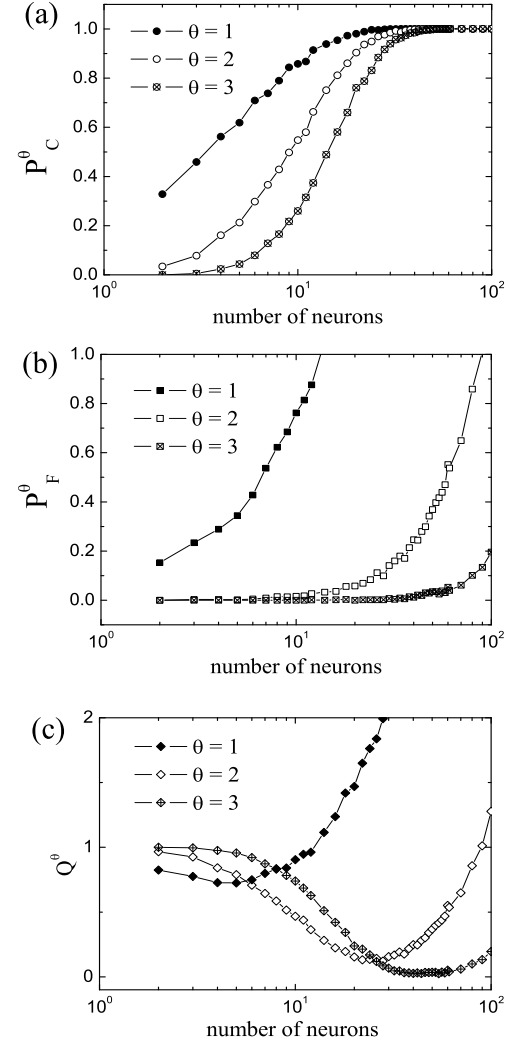


FIG. 7: Detection of subthreshold signals with the network: (a)  $P_C^\theta$  as a function of number of SHH neurons for different coincident detection threshold. (b)  $P_F^\theta$  as a function of number of SHH neurons for different coincident detection threshold. (c)  $Q^\theta$  as a function of number of SHH neurons for different coincident detection threshold.

that the resonance behavior of total error appears again in the network level. Corresponding to different  $\theta$ , there exist different optimal  $N$ . Thus, with this optimal number of neurons, the performance of the network is at its best. And with increasing  $\theta$ , the corresponding optimal  $N$  increases and the total error decreases. Note that when total error is at its minimum, the fraction of correct detection could not reach 1 if coincidence detection threshold is low (for example, see  $\theta = 1$ ). Whereas if  $\theta$  is large, with the network we proposed, the total error could be easily lowered below 0.5.

## V. CONCLUSION

Using a stochastic version of Hodgkin-Huxley neuron model, we investigated the possibility to detection subthreshold signals with channel noise, which is consider as a major source of noise besides the synaptic noise. First, we studies the response property of the SHH neuron to the subthreshold transient input pulses. The main finding is that the response property of SHH neuron to subthreshold pulse input is state dependent. The firing responding to the stimuli as well as the response time depends on the states when the stimuli are applied. The phase plane analysis method is used to investigate the mechanism beneath those phenomena. We also use a pulse detection scenario to evaluate the ability of subthreshold signal detection with channel noise. Through calculating the total error  $Q$  we found that the detection ability of single neuron with channel noise is limited. The same conclusion is obtained by Gregor Wenning, et al.. Therefore, we proposed a possible way of out this predicament, which is detecting the subthreshold signals with synchronous firing of multiple neu-

rons. We found that weak signals can be reliably detected with the strategy we proposed.

We also noticed the phenomenon of stochastic resonance induced by channel noise. This intrinsic stochastic resonance appears both in single neuron level and in network level, indicating that there exist an optimal membrane area for the single neuron and optimal number of neurons for the network to achieve best performance of pulse detection. Since this double-system-size resonance phenomena were rarely reported[24], our work provided an example of such observations.

## Acknowledgements

This work was supported by the National Natural Science Foundation of China under Grant No. 10305005 and by the Fundamental Research Fund for Physics and Mathematic of Lanzhou University.

- 
- [1] D. Paré, E. Shink, H. Gaudreau, A. Destexhe, and E. J. Lang, *J. Neurophysiol.* **79**, 1450(1998).
  - [2] M. Volgushev and U. T. Eysel, *Science*, **290**, 1908(2000).
  - [3] L. Gammaitoni, P. Hanggi, and P. Jung, *Rev. Mod. Phys.* **70**, 223(1998).
  - [4] W. C. Stacey and D. M. Durand, *Engineering in Medicine and Biology*, 1999. 21st Annual Conf. and the 1999 Annual Fall Meeting of the Biomedical Engineering Soc. **1**, 364(1999).
  - [5] W. C. Stacey and D. M. Durand, *J. Neurophysiol.* **83**, 1394(2000).
  - [6] W. C. Stacey and D. M. Durand, *J. Neurophysiol.* **86**, 1104(2001).
  - [7] J. A. White, R. Klink, and A. Alonso, *J. Neurophysiol.* **80**, 262(1998).
  - [8] E. Schneidman, B. Freedman, and I. Segev, *Neural Comput.* **10**, 1679(1998).
  - [9] S. Schreiber, J. M. Fellous, and P. Tiesinga, *J. Neurophysiol.* **91**, 194(2004).
  - [10] E. Schneidman, I. Segev, and N. Tishby, in *Advances in Neural Information Processing*, edited by S. A. Solla, T. K. Leen, and K. R. Miller (MIT Press, Cambridge, 2000). Vol. 12, p. 178.
  - [11] J. A. White, J. T. Rubinstein, and A. R. Kay, *Trends. Neurosci.* **23**, 131(2000).
  - [12] G. Svskis, V. Kotak, D. H. Sanes, and J. Rinzel, *J. Neurophysiol.* **91**, 2465(2004).
  - [13] G. Wenning, T. Hoch, and K. Obermayer, *Phys. Rev. E* **71**, 021902(2004).
  - [14] A. L. Hodgkin and A. F. Huxley, *J. Physiol.* **117**, 500(1952).
  - [15] P. Dayan and L. F. Abbott, *Theoretical neuroscience: computational and mathematical modeling of neural systems*, (USA, MIT press, 2001).
  - [16] S. Y. Zeng and P. Jung, *Phys. Rev. E* **70**, 011903(2004).
  - [17] H. C. Tuckwell and F. Y. M. Wan, *Physica A* **351**, 427(2005).
  - [18] R. VanRullen, R. Guyonneau, and S. J. Thorpe, *Trends. Neurosci.* **28**, 1(2005).
  - [19] S. Boris, G. Gutkin, B. Ermentrout, and D. A. Reyes, *J. Neurophysiol.* **94**, 1623(2005).
  - [20] H. Hasegawa, *Phys. Rev. E* **66**, 021902(2002).
  - [21] G. Svskis, V. Kotak, D. H. Sanes, and J. Rinzel, *J. Neurosci.* **22**, 11019(2002).
  - [22] H. Kitajima and J. Kurths, *Chaos* **15**, 023704(2005).
  - [23] L. M. Ward, *Trends. Cogn. Sci.* **7**, 553(2003).
  - [24] M. S. Wang, Z. H. Hou, and H. W. Xin, *ChemPhysChem* **5**, 1602(2004).